EPR characterisation of the ferrous nitrosyl complex formed within the oxygenase domain of NO synthase.

J. Santolini, Amandine Maréchal, Alain Boussac, Pierre Dorlet

ChemPubSoc Europe

DOI: 10.1002/cbic.201300233

EPR Characterisation of the Ferrous Nitrosyl Complex Formed within the Oxygenase Domain of NO Synthase

Jérôme Santolini,*[a] Amandine Maréchal,[a, b] Alain Boussac,[a] and Pierre Dorlet*[a]

This work is dedicated to the memory of Ivano Bertini for his seminal contribution to the fields of magnetic resonance and bioinorganic chemistry.

Nitric oxide is produced in mammals by a class of enzymes called NO synthases (NOSs). It plays a central role in cellular signalling but also has deleterious effects, as it leads to the production of reactive oxygen and nitrogen species. NO forms a relatively stable adduct with ferrous haem proteins, which, in the case of NOS, is also a key catalytic intermediate. Despite extensive studies on the ferrous nitrosyl complex of other haem proteins (in particular myoglobin), little characterisation has been performed in the case of NOS. We report here a temperature-dependent EPR study of the ferrous nitrosyl complex of the inducible mammalian NOS and the bacterial NOS-like protein from *Bacillus subtilis*. The results show that the overall behaviours are similar to those observed for other haem proteins, but with distinct ratios between axial and rhombic forms in the case of the two NOS proteins. The distal environment appears to control the existence of the axial form and the evolution of the rhombic form.

Introduction

Nitric oxide (NO) is an essential radical molecule that is involved in various physiological processes, ranging from signalling processes to cytotoxic activities.[1] In mammals it is produced by a class of enzymes, the NO synthases (NOSs), through a two-step reaction. In the first step, L-arginine is oxidised to N^{ω}-hydroxyarginine (NOHA); in the second step, this is oxidised to citrulline and NO.[2] Among the various reaction intermediates, the ferrous nitrosyl complex {FeNO}^{7} plays a dominant role. Its formation in the course of NOHA oxidation and its oxidation determine the ability of NOS to release NO.[3] Moreover, it is the starting point of a futile cycle[4] in which the reactivity of the {FeNO}^{7} species controls the balance between NO release and production of reactive nitrogen and oxygen species (RNOS).[5]

The interaction of NO with haemoproteins (e.g., globin,[6] cytochrome *c* oxidase,[7] soluble guanylate cyclase)[8] is crucial in the homeostasis of NO and for its biological impact.[5d,9] As NOSs are the source and the first target of NO, characterisation of the structural and electronic properties of the NOS {FeNO}^{7} complex appear necessary to understand the biology of NO and RNOS. However, only a few spectroscopic characterisations have been performed so far on this species.[10] EPR is one of the most suitable techniques to describe its electronic properties and to investigate its reactivity. Reports have described the EPR fingerprint of NOS {FeNO}^{7} complexes and the influence of the haem distal environment on its geometry.[10a,d] Although the existence of a thermal equilibrium between a rhombic (R) and an axial (A) form has been described for several haemoproteins (including myoglobins, haemoglobins and neuroglobins),[11] the possible existence of such conformers and their respective structures have never been addressed for NOSs or other haemothiolate proteins; despite intensive investigations, the nature of the equilibrium and the identification of the low temperature (A) form remain under debate (see refs. [11d–f] and references therein).

In this context, we decided to investigate the temperature dependence of the NOS {FeNO}^{7} complex. The changes were followed by EPR spectroscopy on two different NOSs: the mammalian inducible NOS (iNOS) and the NOS-like protein from *Bacillus subtilis* (bsNOS), which have been shown to enhance and abolish, respectively, the damaging oxidative reactivity of the potent RNOS peroxynitrite.[12] We analysed the influence of the haem distal environment by varying the nature of the substrate. Our results allow a better analysis of the effect of temperature on the different features of the EPR spectra, and are a novel contribution to the on-going debate over the properties of haem {FeNO}^{7}.

[a] *Dr. J. Santolini, Dr. A. Maréchal, Dr. A. Boussac, Dr. P. Dorlet*
CNRS, UMR 8221, CEA/iBiTec-S/SB^{2}SM
Bât. 532, CEA Saclay, 91191 Gif-sur-Yvette Cedex (France)
E-mail: jerome.santolini@cea.fr
pierre.dorlet@cea.fr

[b] *Dr. A. Maréchal*
Current address: Glynn Laboratory of Bioenergetics
Institute of Structural and Molecular Biology, University College London
Gower Street, London WC1E 6BT (UK)

Results and Discussion

Nitrosyl complex of iNOS

The ferrous nitrosyl complex for the mammalian iNOS was prepared in the presence of substrate (L-arginine) and cofactor (tetrahydrobiopterin, H4B). The EPR spectrum obtained at low

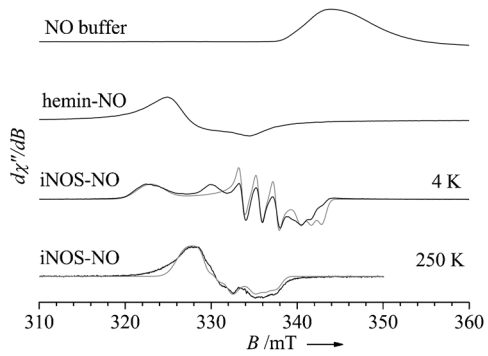

Figure 1. EPR spectra of NO in buffer, and of the ferrous nitrosyl complexes of hemin and iNOS (+H4B/+Arg) at 4 K and 250 K. Spectra in grey are simulations (parameters in Table 1). Experimental conditions: microwave frequency 9.49 GHz (NO buffer), 9.42 GHz (iNOS–NO 4 K, hemin–NO) and 9.38 GHz (iNOS–NO 250 K); microwave power 1 mW (NO buffer, hemin–NO), 0.2 μW (iNOS–NO 4 K) and 0.1 mW (iNOS–NO 250 K); modulation amplitude 0.5 mT (NO buffer, hemin-NO), 0.4 mT (iNOS–NO 4 K) and 0.2 mT (iNOS–NO 250 K); modulation frequency 100 kHz; temperature 10 K (NO buffer, hemin–NO), 4 K (iNOS–NO 4 K) and 250 K (iNOS–NO 250 K).

temperature for this sample is shown in Figure 1 (spectrum iNOS–NO 4 K). Similarly to what has been observed for such complexes in other haem proteins,[11] the spectrum is a mixture of a rhombic powder pattern (R) and a more axial one (A). The R form is characteristic of a six-coordinated species, with hyperfine coupling because of the nitrogen nucleus (^{14}N, $I=1$) of NO, well resolved on the central g value. The simulated spectrum for the rhombic pattern is shown along the experimental spectrum in Figure 1, and the parameters are reported in Table 1. The differences between experimental and simulated spectra above 340 mT might be due to excess NO in solution

Table 1. EPR parameters obtained from the simulation of the experimental spectra for the nitrosyl complexes of iNOS and bsNOS at low and high temperature in the presence of substrate and cofactor.

	bsNOS		iNOS	
	10 K	220 K	4 K	250 K
g (g-strain)	2.081 (0.006)	2.068 (0.017)	2.084 (0.018)	2.047 (0.015)
	2.004 (0.000)	2.009 (0.000)	2.006 (0.001)	2.026 (0.004)
	1.967 (0.004)	1.981 (0.011)	1.970 (0.005)	1.993 (0.005)
A_{14N} (MHz)	29	31	30	10
	58	59	56	37
	33	25	34	35

(Figure 1, top spectrum). The A form has a dominant contribution at $g=2.040$ and is very difficult to characterise, as was the case in previous studies of ferrous nitrosyl complexes.[11d] This form has been routinely observed in the six-coordinated {FeNO}^{7} complex, both in proteins and in model complexes (refs. [11d], [11h] and [13] and references therein). It is noteworthy that this form is clearly distinct from the ferrous hemin nitrosyl complex in solution (Figure 1), and is also different from the five-coordinated {FeNO}^{7} complex within NOS, which displays a characteristic EPR spectrum.[10b,d] These observations have also been reported for the other family of haemothiolate proteins, cytochromes P450 (CYPs).[14] As observed for other ferrous haem nitrosyl complexes in proteins, the EPR spectrum was found to be highly dependent on temperature. The spectrum recorded on the same sample at 250 K (along with a simulated spectrum; Figure 1, bottom spectra) remains rhombic, but its g anisotropy is dramatically reduced, with loss of the hyperfine coupling resolution.

In order to understand the changes observed in these spectra, we recorded EPR spectra of the nitrosyl complex as a function of temperature. Selected spectra are displayed in Figure 2. Because of the large g anisotropy (compared to systems with

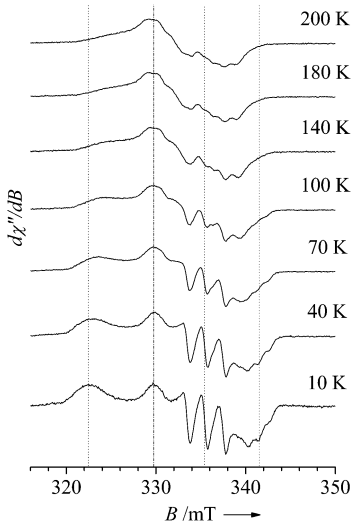

Figure 2. Experimental EPR spectra for iNOS (+H4B/+Arg) nitrosyl complex at the indicated temperatures. Experimental conditions: microwave frequency 9.41 GHz, microwave power 0.2 μW (10 K), 3.2 μW (40 K) and 50.0 μW (100–200 K); modulation amplitude 0.4 mT; modulation frequency 100 kHz. The dotted lines indicate the field positions corresponding to the three principal g values of the lowest temperature spectrum. The dash-dotted line indicates the field position of the additional EPR feature at $g=2.040$ at 10 K.

a proximal histidine, such as myoglobin), it is evident that the g values of the R form here change with temperatures. Clear changes in the spectrum start at around 70 K, with g_{max} (R form) decreasing and g_{mid} and g_{min} increasing with increasing temperature. In addition, these features became significantly broadened as the temperature was increased, thus making the principal g values difficult to determine at 140 K and above. However, we note that the low field edge can still be followed clearly enough, even at higher temperatures. In parallel, the additional feature at $g=2.040$ (dash/dotted line) broadens at 70 K and then seems to split into two at 140 K (and above).

Several models have been proposed to explain the temperature-related evolution of the ferrous nitrosyl complexes of haem proteins, in particular for myoglobin and haemoglobin. Equilibrium between an axial and a rhombic form has been suggested, with the rhombic form dominant at low temperatures.[11c] A second proposition involves two axial forms (in addition to the rhombic one), with one at low temperatures and the other at high temperatures.[15] Finally, multifrequency EPR studies led to the conclusion that the g values of both axial

and rhombic forms were also temperature dependent.[11a,e] Overall, a consensus seems to have emerged, with a model based on equilibrium between rhombic and axial forms and the *g* values of both changing with temperature.[11d,f,g] Such an equilibrium was also suggested in the case of $CYP450_{scc}$ in the presence of cholesterol.[16] In contrast, the temperature dependence observed for the five-coordinated {FeNO}^{7} complex did not display interconversion between the two forms in the case of soluble guanylate cyclase.[8a]

In the present case, {FeNO}^{7} complex of iNOS in the presence of the cofactor and substrate L-arginine, it is clear from the dependence of the *g* values that the rhombic form (dominant at low temperatures) evolves towards a more axial species at high temperatures. In contrast, the evolution of the resonance at $g = 2.040$ at 10 K (attributed to an axial form) is not obvious and is more difficult to follow. Indeed, the observed changes in the $g = 2.040$ region might arise from the appearance of a new powder pattern or from the superimposition of the R and A (low-temperature) forms. As a result, assessment of the ratio between R and A contributions cannot be determined precisely as a function of temperature. In this context, it is not clear whether or not the two forms interconvert.

In a previous study on the proximal environment of a NOS-like protein of the bacterium *B. subtilis*, we reported EPR spectra of the {FeNO}^{7} complex.[10b] In that case, the contribution of the $g = 2.040$ form was found to be negligible at low temperatures. We therefore performed a temperature study of the observed EPR spectrum, and compared the results with those for mammalian iNOS.

Nitrosyl complex of bsNOS

The ferrous nitrosyl complex of the NOS-like protein from *B. subtilis* was prepared in the presence of substrate (L-arginine) and cofactor. The EPR spectrum obtained at low temperature (Figure 3, top spectrum) exhibits a single rhombic pattern with three well-resolved *g* values characteristic of a six-coordinated complex. In addition, and in contrast to what was observed for iNOS, the hyperfine coupling with the nitrogen nucleus of NO was also resolved at all three turning points. The parameters of the simulated spectrum are reported in Table 1. The experimental spectrum recorded at 10 K could be well reproduced by using a single powder pattern, thus showing that a single {FeNO}^{7} species is highly dominant in solution. It is noteworthy that the contribution of the axial form (responsible for the resonance at $g = 2.040$) is negligible here.

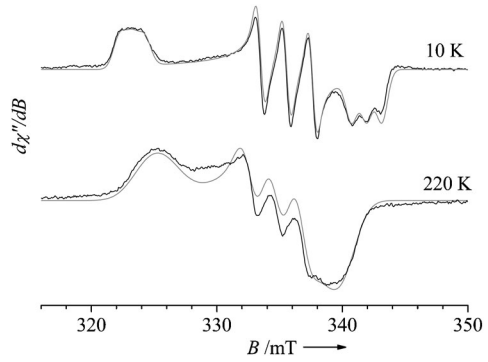

Figure 3. Experimental (black) and calculated (grey) EPR spectra for bsNOS (+H4B/+Arg) nitrosyl complex at 10 K (top) and 220 K (bottom). Experimental conditions: microwave frequency 9.41 GHz; microwave power 1.0 μW (10 K) and 1.6 mW (220 K), modulation amplitude 0.5 mT (10 K) and 0.25 mT (220 K); modulation frequency 100 kHz. Simulation parameters are reported in Table 1.

The EPR spectrum for bsNOS was recorded as a function of temperature. The high-temperature spectrum, recorded on the same sample at 220 K, is also shown in Figure 3 along with its simulated spectrum (bottom spectra). At this temperature, the spectrum remains rhombic, with nitrogen hyperfine coupling still well resolved on the central *g* value resonance, but the line width is broader and the *g* anisotropy is significantly lower than at 10 K. Selected spectra recorded at different temperatures are displayed in Figure 4. Similarly to iNOS, the g_{max} value

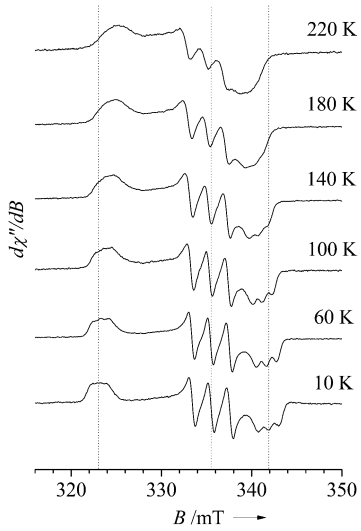

Figure 4. Experimental EPR spectra for bsNOS (+H4B/+Arg) ferrous nitrosyl complex at selected temperatures. Experimental conditions: microwave frequency 9.41 GHz; microwave power 1 μW (10 K), 0.4 mW (60 K and 100 K) and 1.6 mW (140–220 K); modulation amplitude 0.5 mT (10 K) and 0.25 mT; modulation frequency 100 kHz. The vertical dotted lines indicate the field positions corresponding to the three principal *g* values of the lowest temperature spectrum.

decreases while the g_{mid} and g_{min} values increase continuously as the temperature is increased. Within the temperature range 10–60 K, the changes in *g* values are not very significant, and the hyperfine coupling of the nitrosyl nitrogen remains resolved at all three turning points. Changes become more important above 60 K where clear shifts in the g_{max} and g_{min} values are evident. In addition, above 140 K, the hyperfine coupling resolution is lost for the g_{max} and g_{min} features, as the whole spectrum keeps broadening.

Similarly to what has been observed in the case of peroxidases,[11h] the EPR spectrum of the {FeNO}^{7} complex of bsNOS in the presence of cofactor and substrate L-arginine can be considered as a single rhombic powder pattern: specifically, the axial contribution (resonance at $g = 2.040$) was not present in

this sample. There was therefore neither equilibrium nor a conversion between rhombic and axial forms. Only decrease in *g* anisotropy of the rhombic pattern and some line broadening were observed with increasing temperature. This effect can be attributed, at least in part, to fast relaxation of the transition metal as well as dynamics due in particular to the rotation of the NO unit.[17] These observations on bsNOS do not support the existence of equilibrium between the R and A forms, and suggest that the A form could be a degraded version of the nitrosyl complex.

The temperature-dependence patterns of the {FeNO}^{7} EPR spectra clearly differ between iNOS (Figure 2) and bsNOS (Figure 4). Moreover, line broadening with increasing temperature is less pronounced in bsNOS and occurs at higher temperatures. The haem-binding sites in iNOS and bsNOS have high structural homology.[18] However, significant differences between their overall 3D structures remain. In particular, the dimer interface is truncated in the bsNOS protein.[18] Furthermore, the conformational equilibrium between the loose and tight forms—and the parameters that control it—vary among NOS and NOS-like proteins.[19] These differences in the quaternary structure of NOS proteins could partly explain the NOS-dependent effect of temperature on conformational equilibrium of the {FeNO}^{7} species. Additionally, despite an identical catalytic site, the interaction of a distal ligand (NO, CO or O_2) with the L-arginine substrate seems different between bsNOS and iNOS.[10a,d,20] Finally, a conserved valine residue in mammalian NOS on the roof of the haem pocket (modulating haem–NO binding kinetics) is a bulkier isoleucine in bsNOS.[5b,21] These differences might also explain the distinct sensitivities of the {FeNO}^{7} geometries of iNOS and bsNOS to temperature. Thus, we investigated the influence of the nature of the substrate on the {FeNO}^{7} EPR spectrum.

Influence of the presence of substrate

We prepared samples of iNOS with no substrate or with its second natural substrate, NOHA. The corresponding spectra at low, intermediate and high temperatures are shown in Figure 5. In the absence of substrate (top spectra), the lowest temperature spectrum exhibits the characteristic rhombic powder pattern of a six-coordinated nitrosyl complex. The additional feature at 2.040 is also present, although it is less pronounced in this particular sample compared to what was observed in the presence of L-arginine. When the temperature was increased, a similar trend as that seen for iNOS with L-arginine was observed. However, the changes occurred above 120 K (cf. 70 K for iNOS with L-arginine). When NOHA was the bound substrate, {FeNO}^{7} displayed a rhombic EPR signal at 4 K, somewhat different to those observed in the presence or absence of L-arginine: the anisotropy was reduced, and the g_{max} resonance did not exhibit the characteristic triplet shape because of the nitrogen hyperfine coupling. When the temperature was raised, the same trend was observed, but this is harder to follow because of the lower anisotropy: both features rapidly merge over a temperature range similar to that observed with L-arginine as substrate.

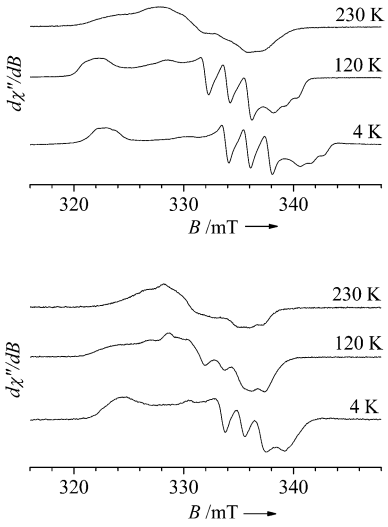

Figure 5. Experimental EPR spectra for iNOS +H4B/no substrate (top) and iNOS +H4B/+NOHA (bottom) ferrous nitrosyl complex at 4 K, 120 K and 230 K. Experimental conditions: microwave frequency 9.42 GHz (4 K) and 9.38 GHz (120 and 230 K); microwave power 0.2 μW (4 K) and 0.13 mW (120 and 230 K); modulation amplitude 0.4 mT (4 K) and 0.2 mT (120 and 230 K); modulation frequency 100 kHz.

The observed changes in the {FeNO}^{7} EPR spectrum with increasing temperature depend on the presence and the nature of the substrate: the proportion of the low-temperature (A) form was highest in the presence of L-arginine, and the emergence of the R form occurred at a lower temperature (below 120 K) in the presence of substrate. This suggests that the substrate and the distal H-bond network control the geometry of the {FeNO}^{7} species. This is reminiscent of what has been described for haemoglobin and neuroglobin. Indeed, the A form of the {FeNO}^{7} species seems favoured by the H-bond interaction between NO and the nitrogen of the distal histidine.[11f,g] Besides, the evolution of the spectrum is observed at higher temperature, when this interaction is suppressed.[11f] In this regard, L-arginine (and to a lesser extent NOHA) could play a similar role in NOS to that in neuro- and haemoglobin (ascribed to the distal histidine). In the case of haemothiolate CYP450s, various situations were encountered, as the proportions of R and A forms depended on the nature of the CYP450, and the substrate could also influence the different components in the EPR spectra.[14,16] As the occurrence of rhombic and axial forms is also observed in model complexes,[13,22] it is not clear what the real cause for the existence of each form is. However, the observations made on CYP450s and NOSs clearly indicate important roles for the distal pocket and the substrate on the structural and electronic properties of the {FeNO}^{7} complex. In the case of NOS, this should be important with respect to the catalytic cycle and the structure–function relationship, as the ferrous nitrosyl moiety is a reaction intermediate during the second step of catalysis.

Conclusions

We investigated the effects of temperature on the {FeNO}^{7} EPR spectra of NO synthases. The larger *g* anisotropy of NOS {FeNO}^{7} signals and the comparative study of two isozymes made the analysis of the evolution of the various forms with temperature easier and allowed assessment of different models. We confirmed that different forms coexist over a large range of temperatures and that the R form experiences a continuous change in its geometry as the temperature increases. In a similar way to that reported for globins, we observed that these two phenomena depend on the interaction of NO with the distal environment and, in this case, with the substrate. However, interconversion of the R and A forms over temperature is not straightforward, and the exact nature of the A form remains in doubt. Comparative analysis of various NOS isoforms by advanced EPR techniques (ESEEM, high-field EPR) appears to be a promising approach to definitively resolve these questions in the case of NOS.

Experimental Section

Chemicals: Chemicals and reagents were purchased from Sigma–Aldrich. Argon and NO gases were purchased from Messer France SA (Asnières, France).

Enzyme preparation: The wild-type iNOS oxygenase domain (iNOS) containing a His_6 tag at its C terminus was expressed in *Escherichia coli* BL21 by using the PCWori vector as previously described.[23] The bacterial NOS-like protein from *B. subtilis* (bsNOS) was overexpressed in *E. coli* BL21 as previously reported.[24] All proteins were purified in the absence of H4B and Arg, by using Ni^{2+}-nitrilotriacetate affinity chromatography as described previously.[25] NOS concentrations were determined by the absorbance at 444 nm of the haem ferrous–CO complex ($\varepsilon_{444}=74\ mM^{-1}cm^{-1}$).

Ferrous nitrosyl complex preparation: iNOS or bsNOS was washed and conditioned in HEPES buffer (100 mM, pH 7.4) in the absence or presence of cofactor H4B (100 μM) and substrate arginine (5 mM) or *N*-hydroxy-arginine (NOHA, 5 mM), depending on the experiment, by three consecutive cycles of dilution/concentration of enzyme (×10) at 4 °C in a Centricon 30 kDa filters (Merck Millipore). Special care was given to the preparation of fresh sodium dithionite solutions to avoid, as much as possible, the presence of degradation products (with consequent loss of dithionite reductive potency). Fresh sodium dithionite (15 mg) was conditioned in a small glass bottle under an inert atmosphere before being dissolved in freshly degassed HEPES (2 mL; 100 mM, pH 7.4), added with an anaerobic Hamilton syringe. To determine the true dithionite concentration, this freshly prepared solution was diluted (×500) in HEPES (100 mM, pH 7.4) containing cytochrome *c*. The difference in absorption ($\varepsilon_{550}=21\,000\ M^{-1}cm^{-1}$) before and after dithionite addition allowed determination of concentration (generally, 20–25 mM). Theoretically, the concentration of such a solution was expected to be ~40 mM. To prepare NO solution, HEPES (2 mL; 100 mM, pH 7.4) was degassed in a small hermetically sealed glass bottle. NO gas, previously washed KOH (0.1 N) to eliminate nitrated NO derivatives, was allowed to bubble in the solution for 5 min. NO concentration was verified by reaction with a solution of oxyhaemoglobin in HEPES (100 mM, pH 7.4). The difference in absorption at 577 and 590 nm (for oxyhaemoglobin and methaemoglobin, respectively), recorded before and after reaction with NO, allowed determination of the concentration of freshly prepared NO-saturated solution ($\Delta\varepsilon_{577-590}=10\,300\ M^{-1}cm^{-1}$); this was found to be ~3.3 mM, in accordance with the literature.[26] iNOS and bsNOS Fe^{III} samples were reduced directly in an anaerobic EPR tube with the freshly prepared dithionite (stoichiometry 1:2.4). After equilibration of the sample (10 min) NO (3 equiv) was added from the saturated NO solution to allow formation of the ferrous nitrosyl complexes. Care was taken to perform this step very slowly, as local NO excess can lead to protein degradation with loss of the proximal thiolate bond. To avoid Fe^{III} contamination in the sample and spectral analysis complication due to a mixture of EPR active species, sodium dithionite (1 equiv.) was finally added to the sample before it was frozen (198 K) in an ethanol/dry ice bath and transferred to in liquid nitrogen (77 K).

EPR spectroscopy: EPR spectra were recorded on an Elexsys 500 X-band spectrometer (Bruker) equipped with a continuous-flow ESR 900 cryostat and an ITC504 temperature controller (Oxford Instruments, Abingdon, UK). Simulations were performed with the Easyspin software package.[27]

Acknowledgements

This work was supported in part by the French Infrastructure for Integrated Structural Biology (FRISBI) ANR-10-INSB-05-01.

Keywords: EPR spectroscopy · heme proteins · nitrosyl complexes · NO-synthases

[1] a) C. Bogdan, *Nat. Immunol.* **2001**, *2*, 907–916; b) L. J. Ignarro, *J. Physiol. Pharmacol.* **2002**, *53*, 503–514.
[2] W. K. Alderton, C. E. Cooper, R. G. Knowles, *Biochem. J.* **2001**, *357*, 593–615.
[3] J. Santolini, *J. Inorg. Biochem.* **2011**, *105*, 127–141.
[4] J. Santolini, A. L. Meade, D. J. Stuehr, *J. Biol. Chem.* **2001**, *276*, 48887–48898.
[5] a) J. Santolini, S. Adak, C. M. Curran, D. J. Stuehr, *J. Biol. Chem.* **2001**, *276*, 1233–1243; b) Z.-Q. Wang, C.-C. Wei, D. J. Stuehr, *J. Inorg. Biochem.* **2010**, *104*, 349–356; c) D. J. Stuehr, J. Santolini, Z.-Q. Wang, C.-C. Wei, S. Adak, *J. Biol. Chem.* **2004**, *279*, 36167–36170; d) J. Tejero, J. Santolini, D. J. Stuehr, *FEBS J.* **2009**, *276*, 4505–4514.
[6] S. Herold, *C. R. Biol.* **2003**, *326*, 533–541.
[7] C. E. Cooper, *Trends Biochem. Sci.* **2002**, *27*, 33–39.
[8] a) A. Gunn, E. R. Derbyshire, M. A. Marletta, R. D. Britt, *Biochemistry* **2012**, *51*, 8384–8390; b) E. R. Derbyshire, A. Gunn, M. Ibrahim, T. G. Spiro, R. D. Britt, M. A. Marletta, *Biochemistry* **2008**, *47*, 3892–3899.
[9] M. P. Schopfer, J. Wang, K. D. Karlin, *Inorg. Chem.* **2010**, *49*, 6267–6282.
[10] a) A. Brunel, J. Santolini, P. Dorlet, *Biophys. J.* **2012**, *103*, 109–117; b) A. Brunel, A. Wilson, L. Henry, P. Dorlet, J. Santolini, *J. Biol. Chem.* **2011**, *286*, 11997–12005; c) F. J. M. Chartier, M. Couture, *Biochem. J.* **2007**, *401*, 235–245; d) C. T. Migita, J. C. Salerno, B. S. S. Masters, P. Martasek, K. McMillan, M. Ikeda-Saito, *Biochemistry* **1997**, *36*, 10987–10992; e) J. Wang, D. L. Rousseau, H. M. Abu-Soud, D. J. Stuehr, *Proc. Natl. Acad. Sci. USA* **1994**, *91*, 10512–10516; f) A. V. Astashkin, B. O. Elmore, L. Chen, W. Fan, J. G. Guillemette, C. Feng, *J. Phys. Chem. A* **2012**, *116*, 6731–6739.
[11] a) M. Flores, E. Wajnberg, G. Bemski, *Biophys. J.* **1997**, *73*, 3225–3229; b) H. Hori, M. Ikeda-Saito, T. Yonetani, *J. Biol. Chem.* **1981**, *256*, 7849–7855; c) R. H. Morse, S. I. Chan, *J. Biol. Chem.* **1980**, *255*, 7876–7882; d) M. Radoul, M. Sundararajan, A. Potapov, C. Riplinger, F. Neese, D. Goldfarb, *Phys. Chem. Chem. Phys.* **2010**, *12*, 7276–7289; e) P. P. Schmidt, R. Kappl, J. Hüttermann, *Appl. Magn. Reson.* **2001**, *21*, 423–440; f) F. Trandafir, S. Van Doorslaer, S. Dewilde, L. Moens, *Biochim. Biophys. Acta Proteins Proteomics* **2004**, *1702*, 153–161; g) A. M. Tyryshkin, S. A. Dikanov, E. J. Reijerse, C. Burgard, J. Hüttermann, *J. Am. Chem. Soc.* **1999**, *121*, 3396–3406; h) T. Yonetani, H. Yamamoto, J. E. Erman, J. S. Leigh, Jr., G. H. Reed, *J. Biol. Chem.* **1972**, *247*, 2447–2455.

[12] A. Maréchal, T. A. Mattioli, D. J. Stuehr, J. Santolini, *FEBS J.* **2010**, *277*, 3963 – 3973.
[13] T. C. Berto, V. K. K. Praneeth, L. E. Goodrich, N. Lehnert, *J. Am. Chem. Soc.* **2009**, *131*, 17116 – 17126.
[14] D. H. O'Keeffe, R. E. Ebel, J. A. Peterson, *J. Biol. Chem.* **1978**, *253*, 3509 – 3516.
[15] E. Wajnberg, M. P. Linhares, L. J. el-Jaick, G. Bemski, *Eur. Biophys. J.* **1992**, *21*, 57 – 61.
[16] M. Tsubaki, A. Hiwatashi, Y. Ichikawa, H. Hori, *Biochemistry* **1987**, *26*, 4527 – 4534.
[17] N. J. Silvernail, A. Barabanschikov, J. T. Sage, B. C. Noll, W. R. Scheidt, *J. Am. Chem. Soc.* **2009**, *131*, 2131 – 2140.
[18] K. Pant, A. M. Bilwes, S. Adak, D. J. Stuehr, B. R. Crane, *Biochemistry* **2002**, *41*, 11071 – 11079.
[19] I. Salard-Arnaud, D. Stuehr, J.-L. Boucher, D. Mansuy, *J. Inorg. Biochem.* **2012**, *106*, 164 – 171.
[20] a) F. J. M. Chartier, M. Couture, *Biophys. J.* **2004**, *87*, 1939 – 1950; b) B. Fan, J. Wang, D. J. Stuehr, D. L. Rousseau, *Biochemistry* **1997**, *36*, 12660 – 12665; c) D. L. Rousseau, D. Li, M. Couture, S.-R. Yeh, *J. Inorg. Biochem.* **2005**, *99*, 306 – 323; d) J. Santolini, M. Roman, D. J. Stuehr, T. A. Mattioli, *Biochemistry* **2006**, *45*, 1480 – 1489.
[21] a) Z.-Q. Wang, C.-C. Wei, M. Sharma, K. Pant, B. R. Crane, D. J. Stuehr, *J. Biol. Chem.* **2004**, *279*, 19018 – 19025; b) E. Beaumont, J.-C. Lambry, Z.-Q. Wang, D. J. Stuehr, J.-L. Martin, A. Slama-Schwok, *Biochemistry* **2007**, *46*, 13533 – 13540.
[22] V. K. K. Praneeth, E. Haupt, N. Lehnert, *J. Inorg. Biochem.* **2005**, *99*, 940 – 948.
[23] R. Gachhui, D. K. Ghosh, C. Wu, J. Parkinson, B. R. Crane, D. J. Stuehr, *Biochemistry* **1997**, *36*, 5097 – 5103.
[24] S. Adak, K. S. Aulak, D. J. Stuehr, *J. Biol. Chem.* **2002**, *277*, 16167 – 16171.
[25] D. K. Ghosh, B. R. Crane, S. Ghosh, D. Wolan, R. Gachhui, C. Crooks, A. Presta, J. A. Tainer, E. D. Getzoff, D. J. Stuehr, *EMBO J.* **1999**, *18*, 6260 – 6270.
[26] a) J. M. Hevel, M. A. Marletta, *Methods Enzymol.* **1994**, *233*, 250 – 258; b) M. E. Murphy, E. Noack, *Methods Enzymol.* **1994**, *233*, 240 – 250.
[27] S. Stoll, A. Schweiger, *J. Magn. Reson.* **2006**, *178*, 42 – 55.

Received: April 12, 2013
Published online on August 13, 2013